



H₅PW₁₀V₂O₄₀/pyridino-SBA-15 as a highly recyclable, robust and efficient inorganic–organic hybrid material for the catalytic preparation of bis(indolyl)methanes

Reza Tayebee^{a,*}, Mostafa M. Amini^b, Farzaneh Nehzat^a, Omid Sadeghi^b, Mahsa Armaghan^b

^a Department of Chemistry, School of Sciences, Hakim Sabzevari University, Sabzevar, Iran

^b Department of Chemistry, Shahid Beheshti University, G.C., Tehran, Iran

ARTICLE INFO

Article history:

Received 3 August 2012

Received in revised form

14 September 2012

Accepted 15 September 2012

Available online 24 September 2012

Keywords:

Hybrid material

Heteropolyacid

Keggin

Bis(indolyl)methane

Synthesis

ABSTRACT

A highly well-organized heterogeneous protocol is developed for the simple synthesis of bis(indolyl)methanes by the effective mediation of an inorganic–organic hybrid material prepared by the chemically anchoring of H₅PW₁₀V₂O₄₀ onto mesoporous silica (SBA-15). Standard characterization data such as XRD, SEM, and FT-IR for the obtained catalyst verified that the ordered hexagonal mesoporous structure of SBA-15 and the Keggin structure of tungstovanadophosphoric acid on pyridine modified SBA-15 surface are preserved. Reusability experiments demonstrated that the active sites on the pyridine modified SBA-15 mesoporous silica retained their structure after several cycles.

© 2012 Elsevier B.V. All rights reserved.

1. Introduction

Heteropolyacids have attracted much attention during the past decade because of their unique ensemble of properties. The Keggin type vanadium substituted polyoxometalates have been recognized as potent catalysts for many catalytic organic transformations. They exhibit great advantages, and their catalytic properties can be tuned by changing the identity of charge-compensating counteractions, hetero-atoms, and framework metal atoms. High solubility of these materials often makes their separation from the reaction mixture difficult. Therefore, immobilization of the heteropolyacid on supports, with high surface area, improves their catalytic performance in various liquid–solid heterogeneous reactions. Although, physical adsorption of heteropolyacids via encapsulation onto various supports and wet impregnation methods facilitated separation of the catalyst from the reaction mixture, however, weak bonding interaction of heteropolyanion with the support leads to partial leaching, especially with polar solvent media [1,2].

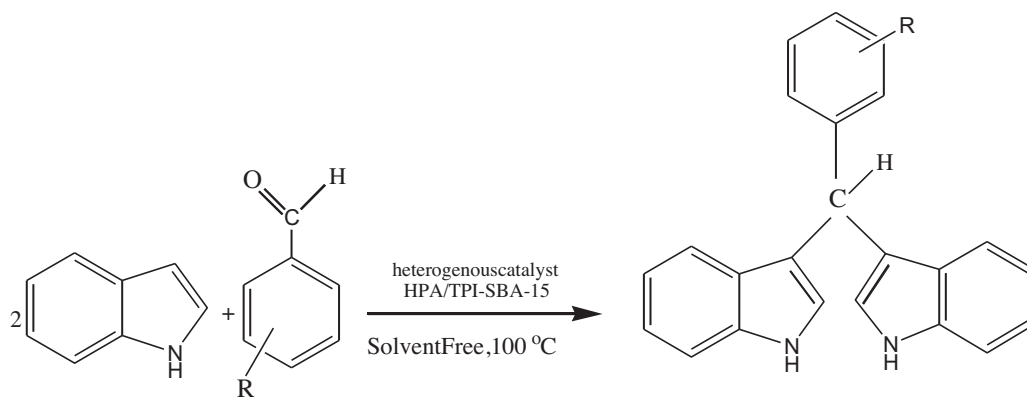
Heterogenizations of heteropolyoxometalates through synthesizing inorganic–organic hybrid materials have been an interesting approach during the past years. This strategy enabled the research

groups to overcome the limitations involved in the separation and recycling of the homogeneous catalysts. Several methodologies have been adopted in the literature for the synthesis of inorganic–organic hybrid materials. Conventionally they are immobilized/anchored on various organic polymers such as resins [3,4], supported on inert porous solids such as alumina and silica [5,6] or encapsulated in the pores and cavities of microporous and mesoporous materials such as zeolites, MCM-41, and SBA-15 [7–9].

As commented, immobilization of homogeneous catalyst onto the porous material through chemical bonding is one of the most powerful strategies to overcome the negative aspects of catalyst leaching. To achieve this goal, it is necessary to use a linker with chemical bonding between catalyst and support. Porous materials have attracted the interest of scientific and technological societies because of their ability to interact with atoms, ions and molecules at surfaces, and forming a basis for the preparation of heterogeneous catalysts. Among various mesoporous molecular sieves, SBA-15 mesoporous silica with uniform channels and narrow pore size distributions has the ability to accommodate some of the huge molecules such as heteropolyanions onto the pores, thus, enable the pore surfaces to be accessed in three dimensions in catalytic reactions [10]. Mesoporous SBA-15 is a more attractive support than X- and Y-type zeolites, and MCM-41 due to its better hydrothermal stability, large pores up to approximately 30 nm, and thick walls [11].

* Corresponding author.

E-mail address: rtayebee@yahoo.com (R. Tayebee).



R=alkyl, halogen,hydroxyl,nitro,methoxy

Scheme 1.

Herein, we wish to study the catalytic activity of different heterogeneous catalysts prepared via wet impregnation method, without chemical bonding, and with inorganic–organic hybrid material synthesized by the chemical anchoring of a linker for the generation of bis(indolyl)methanes. The preparation and characterization of $H_5PW_{10}V_2O_{40}$ immobilized onto amine- and N-[3-(triethoxysilyl)propyl]isonicotinamide (TPI) modified mesoporous silica surfaces (NH_2 -SBA-15 and TPI-SBA-15) are studied, and their catalytic performances are investigated. In this approach, the catalyst HPA/TPI-SBA-15 applied as a highly efficient catalyst for the above condensation reaction (Scheme 1). The heterogeneous nature and reusability of the immobilized catalyst were also studied.

2. Experimental

2.1. Materials and methods

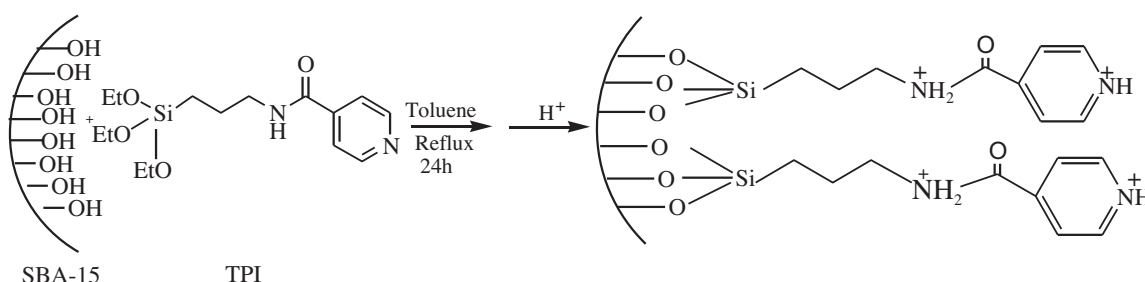
Reagents and starting materials were purchased from commercial resources. All products were identified by comparison of their spectral and physical data with those previously reported [19–23]. Progress of the reactions was monitored by TLC. Infrared spectra were recorded (KBr pellets) on a 8700 Shimadzu Fourier Transform spectrophotometer. 1H and ^{13}C NMR spectra were recorded on a Bruker AVANCE 300-MHz instrument using TMS as an internal reference. Vanadium and molybdenum contents were determined by ICP (Perkin Elmer Plasma 1000 Emission Spectrometer). X-ray diffraction patterns were obtained on a STOE diffractometer with $Cu K\alpha$ radiation. Electron microscopy was performed on a Phillips XL-30 scanning electron microscope (SEM). The heteropolyacid catalyst was prepared and characterized according to the literature procedure [12].

2.2. Synthesis of SBA-15 and pyridine functionalized SBA-15 (TPI-SBA-15)

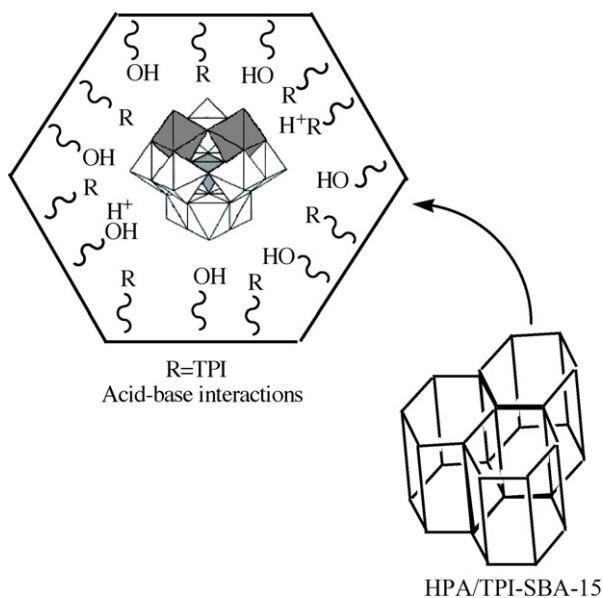
Mesoporous SBA-15 silica was prepared by the method as described elsewhere [13]. For the preparation of pyridine functionalized SBA-15, 1.0 g of SBA-15 was suspended in 50 ml toluene, and the mixture was stirred for 1 h and then 2.0 g of TPI was added and refluxed for 24 h. The white–brownish solid was removed by filtration and was washed with toluene and ethanol and then dried at room temperature. Synthesis of SBA-15 and pyridine-functionalized material (TPI-SBA-15) were confirmed by IR spectroscopy, low-angle X-ray diffraction and elemental analysis. Elemental and thermal analysis of TPI-SBA-15 sample gave pyridine concentration of 1.92 mmol/g. A schematic diagram of modified SBA-15 with TPI is shown in Scheme 2.

2.3. Immobilization of 10-tungsto-2-vanadophosphoric acid on TPI-SBA-15

For immobilization of HPA on TPI-SBA-15, 50 ml of methanol solution containing 0.3 g of $H_5PW_{10}V_2O_{40} \cdot 30H_2O$ was added to a freshly activated TPI-SBA-15 (0.70 g) and the mixture was refluxed for 3 h. Then, the heterogeneous catalyst was filtered and extracted in a soxhlet extractor using methanol as solvent for 12 h and thereafter was dried at 105 °C in a vacuum oven (Scheme 3). The combined filtrate after washing and soxhlation was subjected to UV–vis analysis and found no characteristic bands for tungstodivandophosphoric acid (VHP). This clearly indicated retention of all the VHPA in the pores of TPI-SBA-15. $H_5PW_{10}V_2O_{40}$ loading on TPI-SBA-15 was determined by measuring the amount of tungsten and vanadium in $H_5PW_{10}V_2O_{40}/TPI-SBA-15$ (0.07 mmol/g, 0.20 g/g) by inductively coupled plasma-atomic emission spectroscopy (ICP-AES). Moreover, ICP data clearly confirmed higher



Scheme 2.



Scheme 3.

amount of heteropolyacid is immobilized within the pyridine functionalized support than bare SBA-15. Interestingly, the functionalized mesoporous silica supported HPAs showed no leaching after several hours contact with aqueous solution. The strong interaction between functionalized silica and HPA make it a suitable homogeneous catalyst. As expected, TPI functional group improved immobilization process and higher content of HPA was immobilized within the functionalized support.

2.4. General procedure for the preparation of bis-(indolyl)methanes

A mixture of carbonyl compound (1 mmol), indole (0.234 g, 2 mmol) and the desired amount of the heterogeneous catalyst, as indicated in tables, was stirred at the elevated temperature (100 °C) for the appropriate reaction time. After completion of the reaction, as indicated by TLC, acetonitrile (3 ml) was added to the reaction mixture and the catalyst was filtered off. Then, silica gel (~1 g) was added to the filtrate, and after evaporation of the solvent, a dark pinkish solid mixture was obtained. Purification of the product was performed by a short column chromatography eluted with ethylacetate/petroleum ether (1/9) to give a pinkish solid product in high yields. Products were known compounds and were identified by means of IR and ^1H NMR spectroscopy and/or comparison of their melting points with those reported in the literature.

2.5. Spectral data for selected bis(indolyl)methanes

2.5.1. Bis(indolyl)phenylmethane

^1H NMR (CDCl_3 , 300 MHz), δ (ppm): 5.91 (s, 1H, CH), 6.68 (s, 2H), 7.10 (t, $J=7.3$ Hz, 2H, arom), 7.22 (t, $J=7.3$ Hz, 2H, arom), 7.23 (t, $J=7.2$ Hz, 1H, arom), 7.30–7.40 (m, 2H, arom), 7.35–7.45 (m, 4H, arom), 7.41 (d, $J=7.9$ Hz, 2H, arom), 7.90 (s, br, 2H, NH). ^{13}C NMR, δ (ppm): 40.6, 111.4, 119.7, 120.2, 120.4, 122.4, 124.1, 126.6, 127.5, 128.6, 129.2, 137.1, 144.4. IR (KBr, cm^{-1}) ν_{max} : 760, 820, 890, 960, 1080, 1200, 1410, 1640, 2380, 2880, 2900, 3340.

2.5.2. Bis(indolyl)-4-nitrophenylmethane

^1H NMR (CDCl_3 , 300 MHz), δ (ppm): 5.92 (s, 1H, CH), 6.63 (s, 2H), 6.91 (t, $J=7.3$ Hz, 2H, arom), 7.08 (t, $J=7.3$ Hz, 2H, arom), 7.25 (d, $J=7.9$ Hz, 2H, arom), 7.32 (d, $J=8.1$ Hz, 2H, arom), 7.44 (d, $J=8.6$ Hz, 2H, arom), 8.04 (d, $J=8.6$ Hz, 2H, arom), 9.31 (s, br, 2H, NH). ^{13}C

NMR, δ (ppm): 40.5, 111.8, 117.8, 119.4, 119.7, 122.1, 123.8, 124.4, 127.0, 129.9, 137.3, 146.7, 152.8. IR (KBr, cm^{-1}) ν_{max} : 736, 1086, 1343, 1416, 1457, 1506, 1636, 3447.

2.5.3. Bis(indolyl)-4-chlorophenylmethane

^1H NMR (CDCl_3 , 300 MHz), δ (ppm): 5.82 (s, 1H), 6.54 (brs, 2H), 7.0 (t, 2H), 7.15 (t, 2H), 7.25–7.35 (m, 8H), 7.81 (br, 2H, NH). ^{13}C NMR, δ (ppm): 39.4, 111.2, 129.2, 129.4, 129.8, 122.0, 123.2, 126.4, 128.0, 130.0, 131.4, 136.2, 142.5. IR (KBr, cm^{-1}) ν_{max} : 667, 761, 856, 1012, 1040, 1091, 1124, 1216, 1338, 1416, 1455, 1486, 1518, 1616, 1726, 2853, 2925, 3011, 3056, 3413.

2.5.4. Bis(indolyl)-2,6-dichlorophenylmethane

^1H NMR (CDCl_3 , 300 MHz), δ (ppm): 6.58 (s, 1H), 6.68 (s, 2H), 6.86–7.03 (m, 7H), 7.09 (d, 2H, $J=7.8$ Hz), 7.41 (d, 2H, $J=7.8$ Hz), 7.71 (br, NH). ^{13}C NMR, δ (ppm): 37.2, 110.7, 114.4, 119.3, 119.6, 121.4, 121.8, 124.7, 127.2, 128.2, 128.6, 136.3, 138.7.

2.5.5. Bis(indolyl)-2-nitrophenylmethane

^1H NMR (CDCl_3 , 300 MHz), δ (ppm): 6.12 (s, 1H), 6.91 (s, 2H), 7.08–7.17 (m, 4H), 7.29 (d, 2H, $J=7.8$ Hz), 7.47 (d, 2H, $J=7.9$ Hz), 7.57–7.66 (m, 2H), 7.79–7.90 (m, 2H), 8.21 (d, 2H, $J=8.6$ Hz).

2.5.6. Bis(indolyl)-(1-methyl)methanediyl

^1H NMR (CDCl_3 , 300 MHz), δ (ppm): δ 1.91 (d, 3H, $J=6.8$ Hz), 4.50 (m, 1H), 6.85 (t, 2H, $J=6.8$ Hz), 7.03 (m, 2H), 7.07 (t, 2H, $J=8$ Hz), 7.25 (d, 2H, $J=8$ Hz), 7.40 (d, 2H, $J=8$ Hz), 7.84 (br, 2H). IR (KBr, cm^{-1}) ν_{max} : 3399, 3389, 2958.

2.5.7. Bis(indolyl)-cyclohexanediyl

^1H NMR (CDCl_3 , 300 MHz), δ (ppm): δ 1.61 (m, 6H), 2.54 (m, 4H), 3.25 (m, 1H), 4.60 (s, 1H), 6.89 (t, 2H, $J=7.2$ Hz), 7.07 (m, 4H), 7.29 (d, 2H, $J=8.1$ Hz), 7.55 (d, 2H, $J=8.1$ Hz), 7.92 (br, 2H). IR (KBr, cm^{-1}) ν_{max} : 3450, 3030, 2929, 1658, 1550, 1461, 740.

2.5.8. Bis(indolyl)-3,4-dimethoxyphenylmethane

^1H NMR (CDCl_3 , 300 MHz), δ (ppm): δ 3.76 (s, 3H), 3.85 (s, 3H), 5.83 (s, 1H), 6.65 (d, 2H), 6.78 (d, 2H), 7.0 (t, 3H), 7.17 (t, 2H), 7.29–7.43 (m, 4H), 7.91 (br, NH, 2H). IR (KBr, cm^{-1}) ν_{max} : 3480, 3020, 1604, 1512, 1456, 1418, 1336, 1216, 1091, 1033, 759.

2.5.9. Bis(indolyl)-2-hydroxyphenylmethane

^1H NMR (CDCl_3 , 300 MHz), δ (ppm): δ 3.79 (s, 1H), 5.83 (s, 1H), 6.67 (d, 2H), 6.81 (d, 2H), 7.01 (t, $J=7.2$ Hz, 2H), 7.28–7.46 (m, 6H), 7.92 (br, s, NH, 2H). IR (KBr, cm^{-1}) ν_{max} : 3485, 3021, 2848, 1616, 1517, 1465, 1411, 1326, 1221, 1094.

2.5.10. Bis(indolyl)-2-methoxyphenylmethane

^1H NMR (CDCl_3 , 90 MHz), δ (ppm): 3.82 (s, 3H), 6.32 (s, 1H), 6.61 (s, 2H), 6.81–7.40 (m, ArH, 12H), 7.80 (br, NH, 2H). IR (KBr, cm^{-1}) ν_{max} : 3408, 3056, 2932, 1597, 1486, 1450, 1335, 1102, 745.

2.5.11. Bis(indolyl)-2-chlorophenylmethane

^1H NMR (CDCl_3 , 400 MHz), δ (ppm): 6.34 (s, 1H, Ar-CH), 6.66 (s, 2H), 7.02 (t, 2H, $J=8.0$ Hz), 7.11–7.23 (m, 6H), 7.36–7.43 (m, 4H), 7.96 (br, s, 2H, NH). IR (KBr, cm^{-1}) ν_{max} : 1010, 1037, 1093, 1337, 1417, 1455, 1616, 3052, 3412.

2.5.12. Bis(indolyl)-3-methoxyphenylmethane

^1H NMR (CDCl_3 , 400 MHz), δ (ppm): 3.76 (3H, s), 3.85 (3H, s), 5.83 (1H, s), 6.65 (2H, d), 6.78 (2H, d), 7.0 (3H, t), 7.17 (2H, t), 7.29–7.43 (4H, m), 7.91 (2H, br, NH). IR (KBr, cm^{-1}) ν_{max} : 3480, 3020, 1604, 1512, 1456, 1418, 1336, 1216, 1091, 1033, 759. ^{13}C NMR, δ (ppm): 147.4, 136.7, 127.1, 123.5, 121.9, 119.8, 119.2, 112.3, 111, 55.8, 39.8.

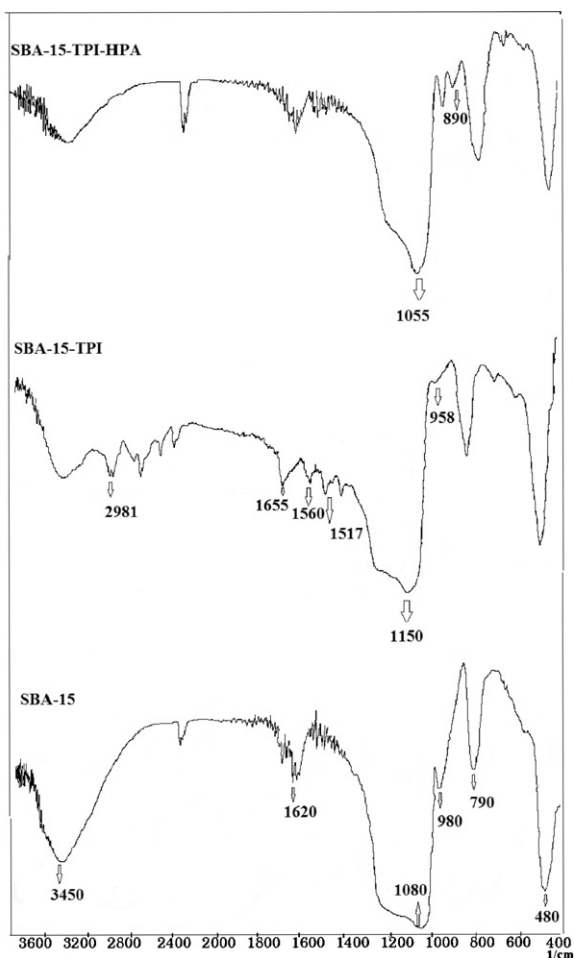


Fig. 1. FT-IR spectra of (A) SBA-15, (B) TPI-SBA-15, and (C) HPA/TPI-SBA-15.

3. Results and discussion

3.1. Structural characterization of the hybrid material

3.1.1. FT-IR spectroscopy

SBA-15 mesoporous silica was functionalized with pyridine by treating with TPI in refluxing toluene. The TPI was anchored to the mesoporous silica surface by condensation of the silanol groups of mesoporous silica and the ethoxy groups of TPI. The incorporation of the pyridine moieties on the mesoporous material was confirmed by FT-IR. The characteristic stretching vibration bands of pyridine at 1655 and 1560 and organosilane at 2981 cm^{-1} in the FT-IR spectra (Fig. 1) of the grafted material confirmed the presence of TPI group on the surface of the mesoporous silica. Furthermore, the Si–O–Si, Si–O and Si–H stretching vibration bands of mesoporous silica appeared at 1060, 958, and 3000–3500 cm^{-1} , respectively. The broad band in the 3500–3700 cm^{-1} region can be attributed to the symmetrical stretching vibration modes of the adsorbed water molecules.

The structure of Keggin HPA anion consists of a PO_4 tetrahedron that surrounded by four W_3O_9 groups formed by the edge sharing octahedron. These groups are connected to each other by corner-sharing oxygen atoms [14]. This structure gives rise to different types of oxygen atoms, being responsible for the fingerprint IR bands of the Keggin anion between 1100 and 500 cm^{-1} (Fig. 2). The four distinct bands belonging to the Keggin structure were centered at 1088, 998, 890, and 778 cm^{-1} [15]. The band at 1088 cm^{-1} was assigned to the symmetric stretching vibration of PO_4 tetrahedron.

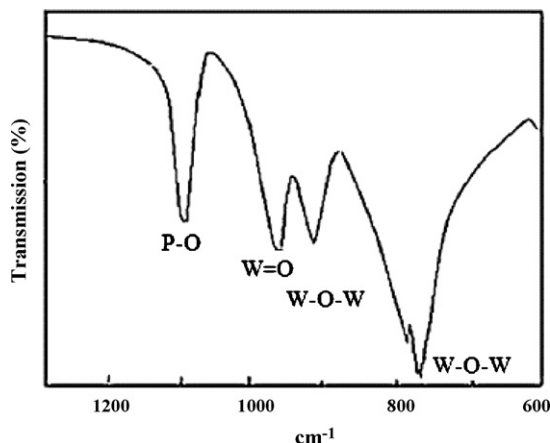


Fig. 2. FT-IR spectrum of $\text{H}_5\text{PW}_{10}\text{V}_2\text{O}_{40}$.

The band at 998 cm^{-1} is due to the stretching vibration of $\text{W}=\text{O}_d$, connecting with the terminal oxygen atoms. The band at 890 cm^{-1} was assigned to the stretching vibration of $\text{W}-\text{O}_b-\text{W}$, associated with corner bridged oxygens, and the band at 778 cm^{-1} comes from the vibration of $\text{W}-\text{O}_c-\text{W}$, associated with side bridged oxygens. From the IR spectrum of HPA/TPI-SBA-15, one can see a broad band in the range of 1000–1250 cm^{-1} , which reveals the strong interaction of silica and heteropolyacid [16]. Actually, clear observation of POM was hindered as a result of the strong background of silica support. Owing to the overlap of the W–O–W and P–O bands with those of Si–O–Si stretching vibrations of mesoporous supports, only the bands corresponding to W–O–W and W–O are discernible after immobilization within the support. Detection of bands related to bulk HPA revealed that the Keggin structure is retained after immobilization. However, a slight shift is evidenced as a result of HPA interaction with functional groups of the support.

3.1.2. X-ray diffraction study

Low-angle powder X-ray diffraction (XRD) patterns of pure, functionalized, and $\text{H}_5\text{PW}_{10}\text{V}_2\text{O}_{40}$ containing SBA-15 are illustrated in Fig. 3. The results showed that the samples are of a high degree of order in a hexagonal close-packed lattice. As can be seen, all patterns showed an intense reflection (1 0 0) at about $2\theta = 1.5^\circ$,

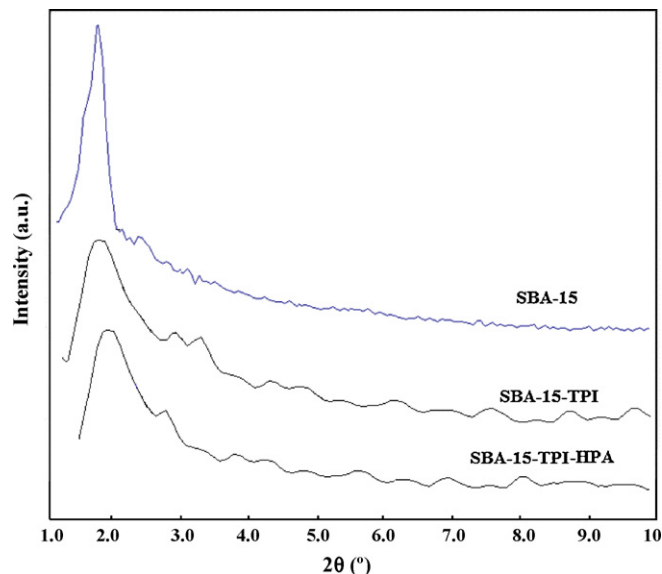


Fig. 3. Low-angle X-ray diffraction patterns of SBA-15, TPI-SBA-15 and HPA/TPI-SBA-15.

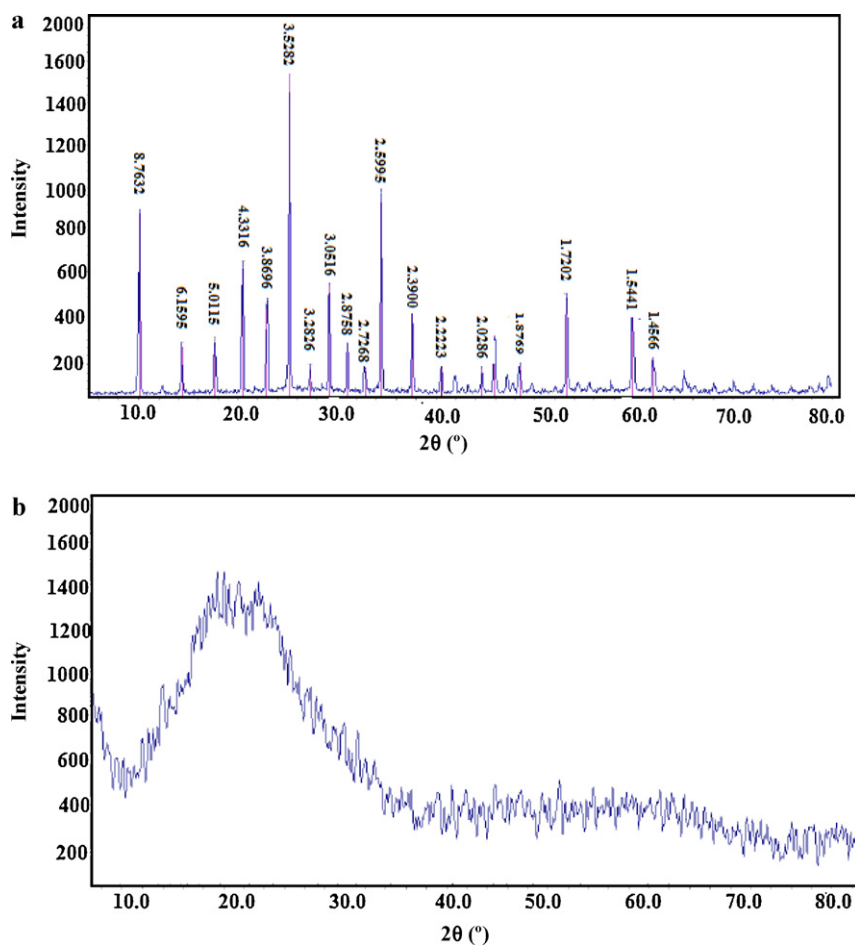


Fig. 4. X-ray diffraction patterns of H₅PW₁₀V₂O₄₀ (a), and H₅PW₁₀V₂O₄₀/TPI-SBA-15 (b).

which indicates that the mesoporous structure of SBA-15 after functionalization with TPI and immobilization of H₅PW₁₀V₂O₄₀ remained intact. The slight shift of the characteristic reflection of SBA-15 in low-angle XRD pattern indicates that the H₅PW₁₀V₂O₄₀ mostly occupied mesoporous channels. Furthermore, for further characterization, the wide-angle XRD patterns of H₅PW₁₀V₂O₄₀ before and after immobilization were recorded (Fig. 4a and b, respectively). The diffraction peaks of H₅PW₁₀V₂O₄₀ with d values of 8.76, 6.15, 5.01, 4.33, 3.87, 3.52, 3.26, 3.05, 2.87, 2.73, 2.60, 2.39, 2.22, 2.03, 1.97, 1.88, 1.72, and 1.54 Å in the 2θ range of 10–80° are in accordance with JCPDS for this compound [17]. Interestingly, the H₅PW₁₀V₂O₄₀ diffraction peaks after incorporation on TPI-SBA-15 collapsed and only a broad peak at about 20° is visible which indicated H₅PW₁₀V₂O₄₀ is well dispersed onto SBA-15 mesoporous silica, and it is a suitable heterogeneous catalyst for a wide variety of catalytic applications. This is in accordance with XRD pattern of heteropolyanions in other supports [17].

3.1.3. SEM studies

The SEM micrographs of TPI-SBA-15 and H₅PW₁₀V₂O₄₀/TPI-SBA-15 are shown in Fig. 5a and b, respectively. SEM micrographs show both materials have similar texture and there is no significant difference and also indicated that the H₅PW₁₀V₂O₄₀ is well dispersed in TPI-SBA-15 and can be used as a heterogeneous catalyst. Furthermore, the intense diffraction at about 2θ = 2° in the low-angle X-ray diffraction patterns of all samples confirmed that the mesoporous structures of SBA-15 after functionalization with TPI and immobilization of HPA are well maintained.

3.2. Studying catalytic activity of some inorganic–organic hybrid materials

Table 1 shows the catalytic activity of some prepared H₅PW₁₀V₂O₄₀ supported inorganic–organic hybrid materials for the synthesis of bis(idolyl)phenylmethane. Clearly, the support material and the amine linker (TPI and/or Pip.) strongly affected the efficacy of the heterogeneous catalyst. The results demonstrated that pyridine-modified SBA-15 is a superior carrier with respect to MCM-41 with the same organic modifier attached to the desired heteropolyacid catalyst H₅PW₁₀V₂O₄₀. The first produced 84% of product after 25 min (entry 2); whereas, the latter yielded the same amount after 60 min (entry 1). Effect of the amine linker on the catalytic efficacy was also investigated. Results revealed that TPI liker (84% after 25 min) behaved distinctly better than NHCl (86% after 150 min, entry 4). Finally, it was found that piperazine linked to NHCl linker supported on SiO₂ (mesh, 230–400, 5–15 μm) activated the heterogeneous catalyst and reduced the reaction time ~50%. The first showed 85% of product after 80 min; whereas, SiO₂-NHCl-H₅PW₁₀V₂O₄₀ produced comparable conversion in 150 min (entry 4).

3.3. Studying the catalytic activity of support material SBA-15 and with TPI linker

Table 2 describes the catalytic activity of H₅PW₁₀V₂O₄₀, TPI-SBA-15, and SBA-15 fragments, separately, in the preparation of bis(indolyl)phenylmethane under the standard reaction condition reported in this work. H₅PW₁₀V₂O₄₀ was solely effective in the

Table 1Comparing the catalytic activity of some prepared inorganic–organic hybrid materials bearing $H_5PW_{10}V_2O_{40}$ for the synthesis of bis(indolyl)phenylmethane.

Entry	Catalyst	Catalyst (g)	$H_5PW_{10}V_2O_{40}$ (mmol)	Time (min)	Yield (%)
1	MCM-41-TPI- $H_5PW_{10}V_2O_{40}$	0.009	10^{-3}	60	84
2	SBA-15-TPI- $H_5PW_{10}V_2O_{40}$	0.02	10^{-3}	25	84
3	SiO_2 -NHCl-Pip- $H_5PW_{10}V_2O_{40}$	0.011	10^{-3}	80	85
4	SBA-15-NHCl- $H_5PW_{10}V_2O_{40}$	0.015	10^{-3}	150	86

Benzaldehyde (1 mmol), indole (2 mmol) and the desired amount of the heterogeneous catalyst, as indicated in table, was stirred at 120 °C for the appropriate reaction time. After completion, the product was worked up as described in Section 2.2.

Table 2Studying the catalytic activity of $H_5PW_{10}V_2O_{40}$, TPI-SBA-15, and SBA-15 in the preparation of bis(indolyl)phenylmethane.

Entry	Catalyst	Catalyst (mg)	Time (min)	Yield (%)
5	$H_5PW_{10}V_2O_{40}$	56	15	84
6	$H_5PW_{10}V_2O_{40}$	3	40	65
7	SBA-15	20	60	55
8	SBA-15-TPI	20	80	45
9	$H_5PW_{10}V_2O_{40}$ /TPI-SBA-15	20	25	84

Reaction condition is described in Section 2.

synthetic route and 0.056 g (2 mol%) of this catalyst produced 84% of product after 15 min (entry 5); whereas, 0.003 g (~0.1 mol%) of this catalyst led to 65% of conversion after 40 min (entry 6). Using inorganic–organic hybrid of $H_5PW_{10}V_2O_{40}$ /TPI-SBA-15 (0.02 g), which was included only 3 mg of the desired heteropolyacid, was

sufficient to obtain 84% of conversion after short time 25 min (entry 9). It is noticeable that free carrier material has also shown some catalytic activity in the desired reaction. SBA-15 and pyridine modified TPI-SBA-15 produced 55 and 45% of conversion after 60 and 80 min (entries 7 and 8, respectively). Obviously, modification of SBA-15 with pyridine decreased its catalytic activity.

3.4. Studying effect of different supporting materials

To compare the role of amine linker on the efficiency of the catalytic system, heterogenization of $H_5PW_{10}V_2O_{40}$ was carried out via physical adsorption on three important carriers including SBA-15, MCM-41, and ZrO_2 (Table 3). These three catalytic systems based on the desired heteropolyacid and carriers were prepared according to the conventional wet-impregnation method. SBA-15, as a mesoporous hexagonal silica with large pores, thick walls, and high hydrothermal stability would act as a promising catalyst support. Furthermore, its large internal surface area allows dispersion of a large number of the catalytically active $H_5PW_{10}V_2O_{40}$. MCM-41 is a class of mesoporous silica tube-like materials with a hexagonal arrangement of uniformly sized one-dimensional mesoporous. This material has high thermal and hydrothermal stability, pores with uniform size and shape, large surface areas, and high hydrophobicity and acidity; therefore, these compounds are of interest as sorbents and solid support in catalysis [18]. According to these comments, results confirmed that SBA-15 is the best carrier and led to 88% yield after 15 min (entry 11). MCM-41 was also effective and produced the same result after somewhat longer time 35 min (entry 12). Notably, ZrO_2 showed the least activity with 71% of conversion after 45 min (entry 13). Meanwhile, homogeneous unsupported $H_5PW_{10}V_2O_{40}$ gave only 50% yield after 40 min (entry 10).

Although, the surface area of $H_5PW_{10}V_2O_{40}$ increases after immobilization onto the solid carriers and good results were obtained, however, leaching of the heteropolyacid during work up by using polar reaction media and poor catalytic reusability of the above physically adsorbed catalysts would be an important limiting problem in practical applications and covalent bonding of the heteropolyacid to the carrier surface via an organic linker would be a promising solution.

To study leaching of $H_5PW_{10}V_2O_{40}$ from the surface of SBA-15, reusability of $H_5PW_{10}V_2O_{40}$ /SBA-15 was investigated. Although this catalyst led to 88% of conversion in the first run after 15 min, however, catalytic efficiency of the protocol was decreased significantly in the next runs by using the recycled $H_5PW_{10}V_2O_{40}$ /SBA-15

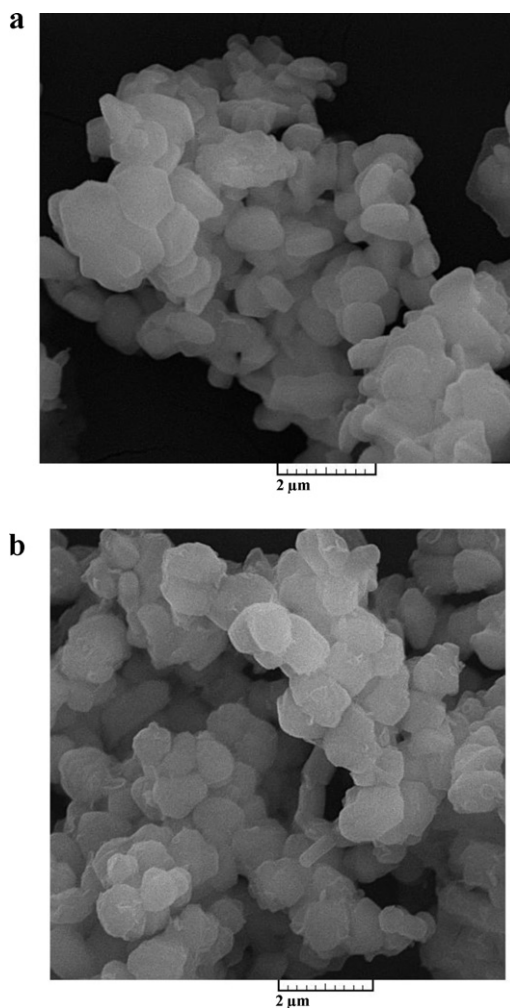


Fig. 5. SEM micrographs of TPI-SBA-15 (a) and $H_5PW_{10}V_2O_{40}$ /TPI-SBA-15 (b).

Table 3

Studying the catalytic activity of some important classical supports obtained via physical adsorption of HPA on the carrier.

Entry	Catalyst (10 mg)	HPA (mmol)	Time (min)	Yield (%)
10	$H_5PW_{10}V_2O_{40}$	10^{-3}	40	50
11	$H_5PW_{10}V_2O_{40}$ /SBA-15	10^{-3}	15	88
12	$H_5PW_{10}V_2O_{40}$ /MCM-41	10^{-3}	35	89
13	$H_5PW_{10}V_2O_{40}$ / ZrO_2	10^{-3}	45	71

Reaction condition is described in Section 2.

Table 4
 Synthesis of various bis(indolyl)methane derivatives in the presence of $H_5PW_{10}V_2O_{40}$ /TPI-SBA-15 under solvent free condition.

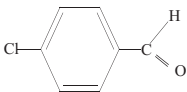
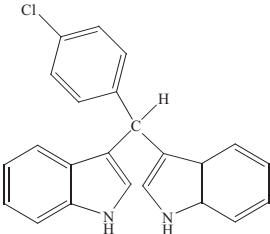
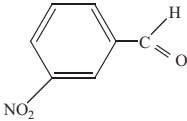
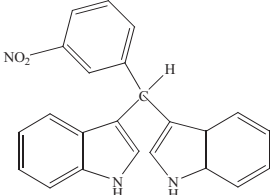
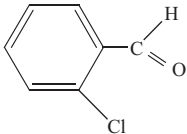
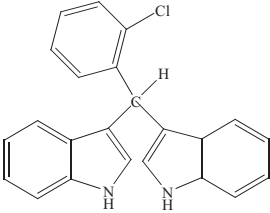
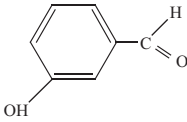
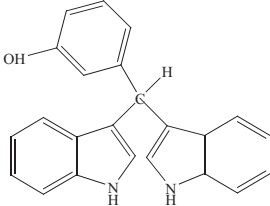
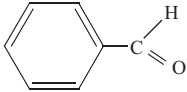
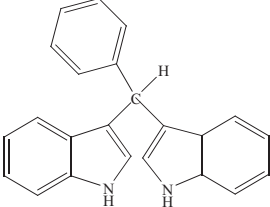
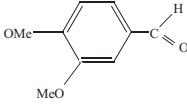
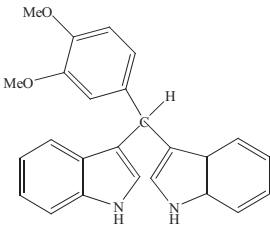
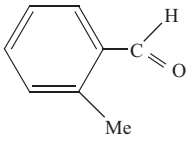
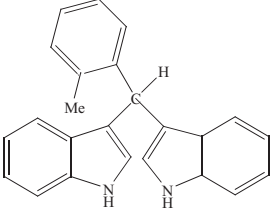
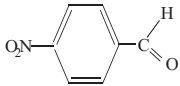
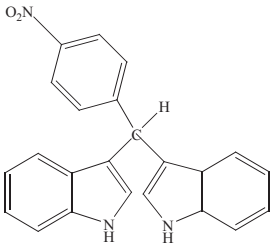
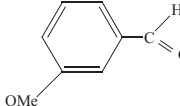
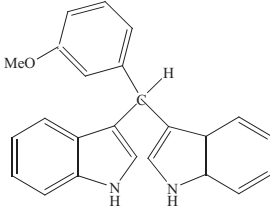
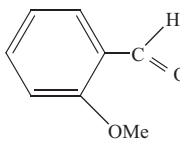
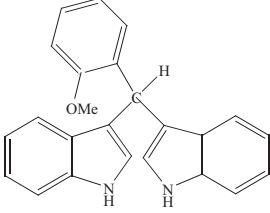
Entry	Substrate	Product	Time (min)	Yield (%)	M.P.	Refs.
14			30	85	76–77	[19]
15			15	95	220–222	[20]
16			20	88	108–109	[20]
17			40	92	98	[21]
18			25	84	149–150	[22]
19			30	75	195	[23]
20			2h	64	95–97	[23]

Table 4 (Continued)

Entry	Substrate	Product	Time (min)	Yield (%)	M.P.	Refs.
21			30	87	217–222	[23]
22			20	78	195	[23]
23			20	66	139–141	[23]

Reaction condition is described in Section 2.

(Fig. 6). This finding clearly proved leaching of the HPA from the surface of SBA-15 during work up as the result of washing the reused catalyst with CH_3CN . Although, leaching problem would be decreased by washing the reused catalyst with less polar solvents, however, $\text{H}_5\text{PW}_{10}\text{V}_2\text{O}_{40}/\text{SBA-15}$ is not a promising proposal for the preparation of the title compounds.

3.5. Synthesis of different bis(indolyl)methanes

In order to prove the applicability of this protocol, a series of structurally diverse aromatic and aliphatic aldehydes bearing electron withdrawing and electron donating substituents were tested in the reaction with indole under standard reaction conditions

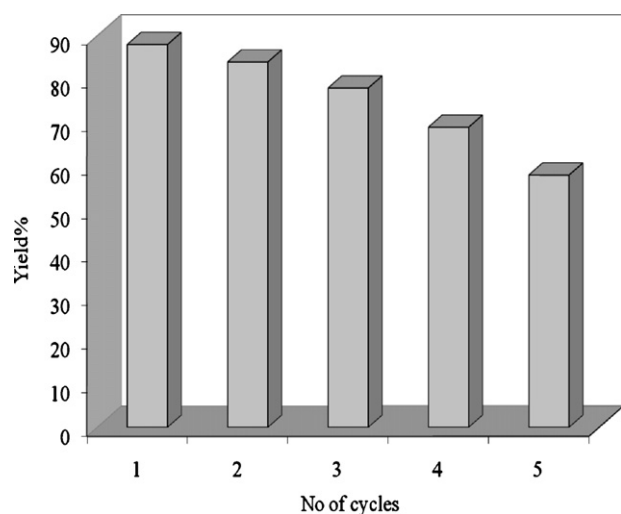


Fig. 6. Reusability study of $\text{H}_5\text{PW}_{10}\text{V}_2\text{O}_{40}/\text{SBA-15}$ in the condensation of benzaldehyde with indole under the optimized reaction conditions.

(Table 4). Findings confirmed that this method is effective for a wide range of aldehydes. However, aldehydes bearing electron withdrawing groups were slightly more effective than aldehydes with electron rich substituents. Aliphatic aldehyde, isopropyl aldehyde, achieved the corresponding bis(indolyl)methane with <35% yields after long time 3 h.

3.6. Comparing the catalytic activity of $\text{H}_5\text{PW}_{10}\text{V}_2\text{O}_{40}/\text{TPI-SBA-15}$ heterogeneous system with other reported catalysts

The superiority of the present protocol was studied over reported methodologies by comparing the obtained results with those reported previously (Table 5). The reaction of benzaldehyde with indole for the synthesis of bis(3-indolyl)methane was selected as a model reaction and the comparison was in terms of mol% of the catalysts, temperature, reaction time, and percentage yields. It seems that the present protocol is superior over reported methodologies considering reaction time, catalyst mol%, ease of work-up, and catalyst recycling.

3.7. Studying reusability of $\text{H}_5\text{PW}_{10}\text{V}_2\text{O}_{40}/\text{TPI-SBA-15}$

In order to prove the reusability of $\text{H}_5\text{PW}_{10}\text{V}_2\text{O}_{40}/\text{TPI-SBA-15}$, it was separated from the reaction mixture and washed with CH_3CN . The catalyst was dried and activated in a vacuum oven for 4 h. The recycled catalyst was reused for a new reaction with benzaldehyde. The catalyst was found to be reusable for at least 10 cycles without considerable loss of activity (Fig. 7). The chemical binding of $\text{H}_5\text{PW}_{10}\text{V}_2\text{O}_{40}$ to the surface of solid support by the mediation of the TPI linker is responsible for the high reusability of the catalyst. Apparently, besides the surface area, particle size, pore structure and distribution of the protons of HPAs, which are usually referred to as the elements of tertiary structure [27], the nature of supports

Table 5
Comparison of the catalytic efficiency of $H_5PW_{10}V_2O_{40}/TPI-SBA-15$ heterogeneous system with some reported catalysts.

Entry	Catalyst	Catalyst mol%	Time	Yield (%)	Condition	Refs.
24	$H_5PW_{10}V_2O_{40}/TPI-SBA-15$	10^{-3}	25 min	84	Solvent free/100 °C	This work
25	$H_6P_2W_{18}O_{62}$	2	15 min	>80	Solvent free/120 °C	[23]
26	$ZrOCl_2 \cdot 8H_2O$	5	40 min	84	Solvent free/50 °C	[24]
27	TiO_2 (nano)	10	12 h	64	$CH_2Cl_2/r.t$	[25]
28	$LiClO_4$	10	5 h	90	$CH_3CN/r.t$	[26]
29	$La(PFO)_3$	5	30 min	90	$CH_3CN/r.t$	[19]

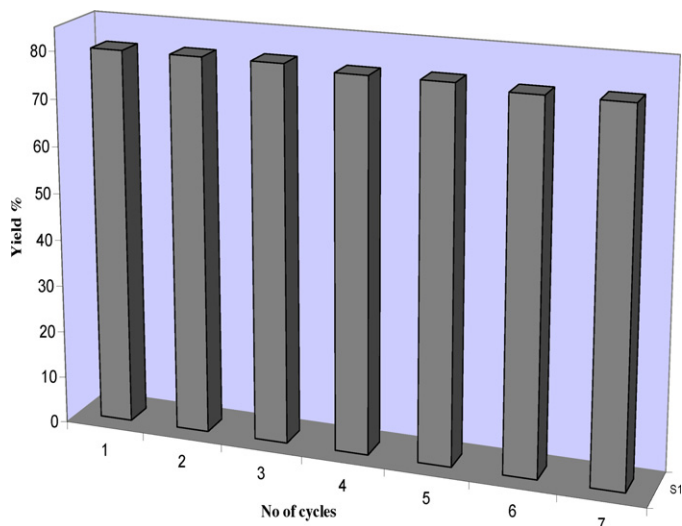


Fig. 7. Yield% as a function of reusability of $H_5PW_{10}V_2O_{40}/TPI-SBA-15$ in the condensation of benzaldehyde with indole under the optimized reaction conditions.

and interaction of HPAs with support is very influential on catalytic activity.

4. Conclusions

A two-step synthesis has been employed to synthesize a new type of $H_5PW_{10}V_2O_{40}$ on TPI functionalized SBA-15. Evidence for the chemical bonding of the heteropolyacid clusters to the SBA-15 surface was provided by several analytical techniques. The pyridine group anchored on the SBA-15 surface and heteropolyacid clusters dispersed well on the TPI-functionalized SBA-15 surface through strong bond. The major advantages of the supported HPA cluster over pure homogeneous HPA were the increased reactivity of the inorganic–organic hybrid material, easy separation, high reusability, and fast recovery of the material.

Acknowledgements

Partial financial support from the Research Councils of Hakim Sabzevari University and Shahid Beheshti University is greatly appreciated. Special thanks to Vahid Tayebee for English editing of the manuscript.

References

- [1] M. Faraj, C. Hill, *J. Chem. Soc. Chem. Commun.* (1987) 1487.
- [2] J.M. Thomas, *Nature* 314 (1985) 669.
- [3] D.C. Bailey, S.H. Langer, *Chem. Rev.* 81 (1981) 109.
- [4] D.E. Devos, P.A. Jacobs, *Catal. Today* 57 (2000) 105.
- [5] M.J. Naughton, R.S. Drago, *J. Catal.* 155 (1995) 383.
- [6] J.P. Arhancet, M.E. Davis, J.S. Merola, B.E. Hanson, *Nature* 339 (1989) 454.
- [7] G.A. Ozin, C. Gil, *Chem. Rev.* 89 (1989) 1749.
- [8] R. Grommen, P. Manikandan, Y. Gao, T. Shane, J.J. Shane, R.A. Schoonheydt, B.M. Weckhuysen, D. Goldfarb, *J. Am. Chem. Soc.* 122 (2000) 11488.
- [9] E. Byambajav, Y. Ohtsuka, *Appl. Catal. A: Gen.* 252 (2003) 193.
- [10] J. Parmentier, S. Saadhallah, M. Reda, *J. Phys. Chem. Solids* 65 (2004) 139.
- [11] F. Ying, J. Li, C. Huang, W. Weng, H. Wan, *Catal. Lett.* 115 (2007).
- [12] E.R. Cadot, A.T.M. Thouvenot, G. Herve, *Inorg. Chem.* 31 (1992) 4128.
- [13] D. Zhao, Q. Huo, J. Feng, B.F. Chmelka, G.D. Stucky, *J. Am. Chem. Soc.* 120 (1998) 6024.
- [14] M.T. Pope, *Heteropoly and Isopoly Oxometalates*, Springer-Verlag, Berlin, 1983, p. 8.
- [15] P. Karandikar, K.C. Dhanya, S. Deshpande, *Catal. Commun.* 5 (2004) 69.
- [16] H.-J. Kim, Y.-G. Shul, H. Han, *Appl. Catal. A: Gen.* 299 (2006) 46.
- [17] A. Tarlani, M. Abedini, A. Nemat, M. Khabaz, M.M. Amini, *J. Colloid Interface Sci.* 303 (2006) 32.
- [18] Q.-Y. Liu, W.-L. Wu, J. Wang, X.-Q. Ren, Y.-R. Wang, *Micropor. Mesopor. Mater.* 76 (2004) 51.
- [19] L. Wang, J.H. Han, T. Sheng, J.Z. Fan, X. Tang, *Synlett* (2005) 337.
- [20] N. Azizi, L. Torkian, M.R. Saidi, *J. Mol. Catal. A: Chem.* 275 (2007) 109.
- [21] S. Sobhani, *J. Organomet. Chem.* 694 (2009) 3027.
- [22] O.R. Sullivan, *Chem. Ind.* (1972) 849.
- [23] A. Kamal, A.A. Qureshi, *Tetrahedron* 19 (1963) 513.
- [24] H. Firouzabadi, N. Iranpoor, A.M. Jafarpour, A. Jafari, *J. Mol. Catal. A: Chem.* 253 (2006) 249.
- [25] M.L. Kantam, S. Laha, J. Yadav, B. Sreedhar, *Tetrahedron Lett.* 47 (2006) 6213.
- [26] J.S. Yadav, B.V. Subba Reddy, V.S.R. Murthy, G. Mahesh Kumar, C. Madan, *Synthesis* (2001) 783.
- [27] E. Rafiee, Z. Zolfaghari, M. Joshaghani, S. Eavani, *Appl. Catal. A: Gen.* 365 (2009) 287.